

Continuous measurement of m -parameter for Hart analysis of superplastic behaviour of ultra-fine grained AZ31 Mg alloy

J. Stráský, J. Stráská, M. Janeček[†]

[†]janecek@met.mff.cuni.cz

Department of Physics of Materials, Faculty of Mathematics and Physics, Charles University in Prague,
Ke Karlovu 5, 121 16 Praha, Czech Republic

The ultra-fine grained materials (UFG) often show superplastic behaviour at elevated temperatures due to small grain size. On the other hand, UFG microstructure is often not stable at increased temperatures and undergoes recovery and recrystallization. In this paper, we investigate the superplastic properties of UFG AZ31 Mg alloy prepared by equal channel angular pressing. The computer controlled tensile tests were performed in a temperature range of 175°C–250°C and at strain rate around 10^{-4} s^{-1} . The superplastic behaviour and strain hardening is related to temperature, strain-rate and microstructure stability. Methodology of continuous measurement of m -parameter during the tensile test to achieve the dependence of m -parameter on true strain is presented. The measurement is based on alternating two slightly different true strain rates, keeping the overall true strain-rate constant. The m -parameter decreases with true strain for all studied conditions from approx. 0.5 to 0.3 and the decrease is fastest for the highest considered temperature (250°C), which is attributed to recovery and recrystallization. The sample deformed at 250°C strain hardens over significantly shorter interval of true strain which also suggests microstructure changes. Limits of plastic instability according to Hart analysis were computed for all conditions. Hart analysis of stability of plastic deformation seems not to be sufficient for description of elongation until fracture for studied material.

Keywords: superplastic behaviour, plastic instability, m -parameter, ultra-fine grained, magnesium alloy

Непрерывное измерение параметра m для анализа Харта сверхпластического поведения ультрамелкозернистого магниевого сплава AZ31

Ультрамелкозернистые (УМЗ) материалы часто демонстрируют сверхпластическое поведение при повышенных температурах благодаря малому размеру зерен. С другой стороны, УМЗ микроструктура часто нестабильна при высоких температурах и испытывает возврат и рекристаллизацию. В данной работе мы исследуем сверхпластические свойства УМЗ магниевого сплава AZ31, подвергнутого равноканальному угловому прессованию. Были проведены управляемые компьютером испытания в температурном интервале 175°C–250°C при скорости деформации около 10^{-4} с^{-1} . Сверхпластическое поведение и упрочнение связаны с температурой, скоростью деформации и стабильностью микроструктуры. Представлена методология непрерывного измерения параметра m во время испытаний растяжением для получения зависимости параметра m от истинной деформации. Измерение основано на чередовании двух незначительно различающихся скоростей деформации при сохранении средней истинной скорости деформации постоянной. Параметр m для всех исследованных случаев уменьшается с увеличением истинной деформации приблизительно от 0.5 до 0.3, и уменьшение наиболее интенсивно для наиболее высокой исследованной температуры (250°C), что связано с возвратом и рекристаллизацией. Образец, деформируемый при 250°C, упрочняется за значительно более короткий интервал истинной деформации, что также говорит об изменении микроструктуры. Для всех состояний рассчитаны пределы пластической нестабильности в соответствии с анализом Харта. Для исследованного материала анализ Харта стабильности пластической деформации представляется недостаточным для описания удлинения до разрушения.

Ключевые слова: сверхпластическое поведение, пластическая нестабильность, параметр m , ультрамелкозернистый, магневый сплав

1. Introduction

It is well known that superplastic behaviour depends on the microstructure, namely the on grain size and also on other factors affecting the diffusivity including dislocation density [1]. The ultra-fine grained materials (UFG) are therefore promising candidates and their enhanced superplastic behaviour was reported in countless studies including those on hexagonal materials [2,3]. The disadvantage of UFG materials is that their microstructure is often not stable at increased temperatures. Therefore, we face interplay, in which increased forming temperature generally causes higher diffusivity, but also microstructure recovery and recrystallization, which may negatively affect the superplastic behaviour. Recovery and recrystallization might occur even during the tensile test and affect the m -parameter elucidation.

In this paper, we investigate the superplastic properties of UFG AZ 31 Mg alloy similarly as many authors in the past [4–7]. The superplastic behaviour is related to microstructure stability at increased temperature, which was investigated in detail in our previous study [8]. The effect of forming temperature on superplastic behaviour and strain hardening is discussed using Hart methodology [9] performed for UFG Mg alloy by Figueiredo and Langdon [3]. The plastic instability is determined by Considère criterion [10] as the lowest ε , for that holds $\theta(\varepsilon) < \sigma(\varepsilon)$, where ε is true strain, σ is true stress and θ is strain hardening computed as:

$$\theta(\varepsilon) = \frac{d\sigma(\varepsilon)}{d\varepsilon}. \quad (1)$$

As pointed out by Hart [9], if the material presents strain-rate sensitivity, the plastic stability is extended due to the fact that actual strain rate at the smallest cross-section is increased. The extended plastic stability limit can be expressed by modifying the strain hardening coefficient:

$$\theta_{Hart}(\varepsilon) = \frac{\frac{d\sigma(\varepsilon)}{d\varepsilon}}{1 - m(\varepsilon)}. \quad (2)$$

Note that the actual value of m -parameter for given ε is required, which is usually unavailable and single m value measured for high strains is considered [3].

In this paper, we present a methodology for continuous measurement of m -parameter during the tensile test at given temperature around given strain rate. The dependence of m -parameter on true strain (and therefore also on time) is achieved.

2. Experimental material and methodology

As-cast commercial AZ31 alloy (nominal composition of Mg-3%Al-1%Zn) was firstly extruded at 350°C with an extrusion ratio of 22 and then processed by 4 passes of equal channel angular pressing (ECAP) with outer angle 90° at 180°C using route B_c with the velocity of 50 mm/min. The angle Φ between two intersecting channels and the corner angle Ψ is equal to 90° and 0°, respectively. The feed-in and exit channels have a square cross section of 10×10 mm. The ECAP die is equipped with an ejector that allows pushing

the sample out of the die immediately after pressing from the feed-in channel to the exit channel. All the specimens were pressed four-times through the ECAP die.

Flat specimens for tensile tests were machined and cut from a single ECAP billet. The length of active part was 16 mm; the thickness and width were approximately 1 and 4 mm, respectively.

Tensile tests were performed using a screw-driven Instron 5882 machine at 175, 200 and 250°C. Computer operated machine allows arbitrary control of t-bar movement. We employed very special strain-rate control. Two different true strain-rates were selected: $\dot{\varepsilon}_1 = 0.9 \times 10^{-4} \text{ s}^{-1}$ and $\dot{\varepsilon}_2 = 1.2 \times 10^{-4} \text{ s}^{-1}$. The actual true strain-rate is switched every two minutes (*i.e.* after $\varepsilon \approx 1.2\%$) during the experiment. Note that the overall t-bar speed is exponentially increased to maintain the two true strain-rates. Therefore, overall true strain dependence is proportional to time dependence ($\varepsilon = 100\% \sim t = 3\text{h}$).

Due to the strain rate sensitivity of the material, the resulting flow curve has a serrated character as shown in Fig. 1 for two different samples (thin serrated curves)¹.

After each strain-rate increase, the actual stress is immediately increased to a higher value. Two minutes ($\varepsilon \approx 1.2\%$) are sufficient to reach the stabilization allowing determination of the stress evolution associated with higher strain-rate. Conversely, after the strain-rate decrease, the stress immediately decreases and its evolution adjusts to the new strain-rate. The parts associated to stabilized stress evolution at higher strain-rate (local maxima) were joined by a smooth curve². Similar-

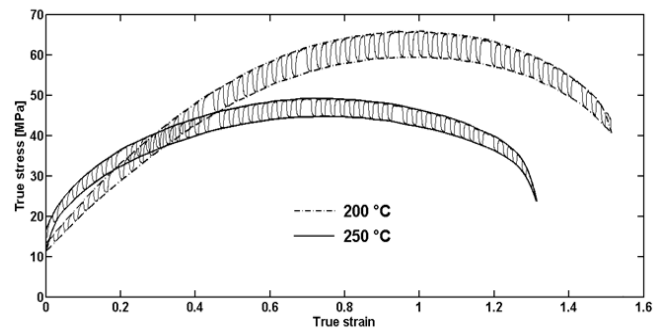


Fig. 1. Measured flow curves for alternating strain-rates (thin serrated curves) and flow curves interpolated through local maxima and minima (thick smooth curves) for samples deformed at 200°C (dashed curves) and 250°C (solid curves).

¹ Technically, average line is first computed from the data by moving average (not shown in Fig.1, but shown in Fig. 3). The relative deviations of measured data from the mean line are employed to identify maxima (and minima). These maxima (and minima) are then interpolated using cubic spline interpolation (in-built procedure in Matlab R2010b).

² Few irregularities (longer regions with higher stress *i.e.* at higher strain-rate) in the serrations are present. These are caused by a mistake in programming of the t-bar movement control. Unintentionally, it is therefore shown that the standard time period (2 mins) between alternations of the strain rate is sufficient. Note that too short time period would lead to underestimated changes of stress with changing strain rate and therefore to underestimation of m -parameter values.

ly, the local minima were interpolated. As a result, we get two flow curves for two strain-rates for a single sample as shown by thick smooth lines in Fig. 1. Therefore, the evolution of m-parameter with strain can be calculated as:

$$m(\varepsilon) = \frac{\ln(\sigma_2(\varepsilon)) - \ln(\sigma_1(\varepsilon))}{\ln(\dot{\varepsilon}_2) - \ln(\dot{\varepsilon}_1)} \quad (3)$$

Note that the denominator is given only by selected strain-rates and is constant.

3. Results

The testing samples were deformed in tension at 175°C (2 samples), 200°C (2 samples) and 250°C (1 sample) according to above described methodology. The measured true stress – true strain flow curves for 200°C and 250°C are shown in Fig. 1. The flow curve for sample deformed at 200°C shows long strain hardening and significant necking at $\varepsilon \approx 144\%$, which corresponds to elongation $\approx 320\%$. The flow curve for 250°C surprisingly shows slightly higher strength values in the beginning of the deformation, but much lower strain hardening. The stable achieved true strain is reduced to $\varepsilon \approx 122\%$ (elongation $\approx 240\%$).

Computed m-parameter evolution with true strain for all investigated samples is shown in Fig. 2. In the beginning of deformation, the m-parameter slightly exceeds 0.5, which is often considered as a lower limit of superplastic behaviour [11] and then decreases with increasing true strain to values just above 0.3, which is considered as a superplasticity limit by other authors [12,13]. The m-parameter for 250°C drops almost at the beginning of the deformation and is significantly lower during the course of deformation.

Fig. 3 shows the flow curves for all three investigated conditions with typical shape showing strain hardening followed by some softening and necking. These flow curves were computed as the average (middle line) of

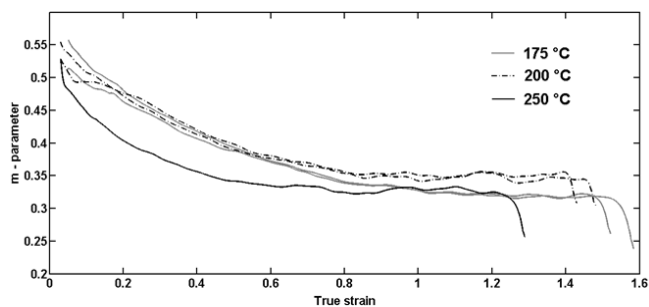


Fig. 2. Evolution of m-parameter computed from interpolated flow curves for samples deformed at 175°C (gray solid curves), 200°C (dashed curves) and 250°C (black solid curve).

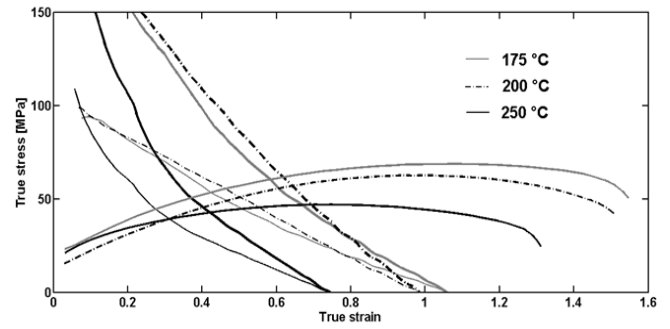


Fig. 3. Flow curves for samples deformed at 175°C (gray solid curves), 200°C (dashed curves) and 250°C (black solid curve). Decreasing curves represent $\theta_{(e)}$ and $\theta_{Hart(e)}$ computed according to Eqs. 1 and 2, where the latter is represented by a thicker line and is shifted to the right compared to its counterpart.

minimum and maximum (lower and higher strain rate) flow curves represented in Fig 1. The flow curves therefore approximately correspond to deformation at strain-rate $\dot{\varepsilon} = 0.9 \times 10^{-4} \text{ s}^{-1}$. The decreasing curves represent $\theta(\varepsilon)$ and $\theta_{Hart}(\varepsilon)$ computed according to Eqs. 1 and 2, where the latter is represented by a thicker line and is shifted to the right compared to its counterpart. Both expressions of strain hardening must obviously meet at $\theta = 0$. The intersections of strain hardening curves with appropriate flow curve are important for determination of plastic stability limit. The values of these intersection points are summarized in Table 1.

The stability limit for 250°C is achieved for much lower strains, which is caused by limited strain hardening at intermediate strains. The strains achieved during instable plasticity are comparable for all temperatures.

4. Discussion

The computed m-parameter values are at the bottom limit to conclude that the alloy exhibits superplastic behaviour [12].

Increased temperature generally increases the diffusion processes, which promote the superplastic behaviour. However, the creep behaviour is also enhanced by fast diffusion paths like pipe diffusion along dislocations or grain boundaries, which might be dominant diffusion processes due to highly deformed UFG microstructure [14,15]. Note also that activation energy of grain boundary diffusion in pure Mg (92 kJ/mol [16]) is much lower than the activation energy of self-diffusion (135 kJ/mol [16]). The decrease of m-parameter for 250°C is therefore probably caused by disappearing of fast diffusion paths possibly due to recovery of dislocation walls reducing the Cobble creep and also due to grain growth, which limits superplastic behaviour according to classical

Table 1. Plastic stability limits according to Eq. 1 and Eq. 2 (Hart analysis) and appropriate true strain in stability and instability ranges

Temperature	$\theta = \sigma$	$\theta_{Hart} = \sigma$	ε_{stable}	$\varepsilon_{unstable}$	$\varepsilon_{Hart\ stable}$	$\varepsilon_{Hart\ unstable}$
175°C	54 MPa	61 MPa	0.42	1.17	0.57	1.02
200°C	49 MPa	55 MPa	0.46	1.06	0.60	0.92
250°C	38 MPa	42 MPa	0.29	1.02	0.40	0.91

Ashby-Verrall model [17]. Limited work hardening at 250°C is also attributed to recovery processes, which occur during static annealing 250°C [8,18]. The grain growth during the tensile test is a topic for further investigation, but the grain growth might be even faster under dynamic conditions [11]. Possible effect of annealing twins observed in [8,18] for annealing temperature of 250°C remains unclear. On the other hand, during annealing at 175°C and 200°C limited decrease of dislocation density was observed [8] and the *m*-parameter decreases more slowly. The *m*-parameter during deformation at 200°C remains higher than at 175°C (possibly due to simple temperature effect on diffusion). This suggests that 200°C is the optimal temperature for interplay between the temperature effect on superplastic behaviour and the microstructure stability in low-temperature low-strain-rate superplasticity.

Hart analysis of plastic stability clearly postpones the plastic instability limit compared to Considère criterion [10]. At 250°C, the limit of stability is achieved for significantly lower strain, which is attributed to limited strain hardening, arguably due to recovery processes. On the other hand, the achieved strain in instability region is very similar for all tested conditions $\varepsilon \approx 100\%$ disregarding the differences in *m*-parameter. Significant strain achieved for all conditions in the expected plastic instability region reported also in [3] limits the utilization of Hart analysis. For instance, at 175°C slightly higher total elongation to fracture than at 200°C was observed, despite both the *m*-parameter and the plastic instability limit were lower. For future works, it is suggested to investigate other models of plastic instability presented by Molinari [19] or Haehner [12].

5. Conclusions

The main results of presented study can be summarized as follows:

The methodology for continuous estimation of *m*-parameter was developed and presented.

m-parameter decreases with true strain for all studied conditions and the decrease is faster for the highest temperature (250°C), which is attributed to recovery and recrystallization.

Limits of plastic instability according to Hart analysis were computed. However this analysis seems to be insufficient for the description of elongation till fracture.

Acknowledgements. This work was financially supported by Czech Science Foundation GACR under the grant 14-36566G.

References

1. Y. Umakoshia, W. Fujitania, T. Nakanoa, A. Inoueb, K. Ohterac, T. Mukaid, K. Higashie. *Acta Materialia* **46** (13), 4469 (1998).
2. R.B. Figueiredo, M. Kawasaki, C. Xu, T.G. Langdon. *Materials Science and Engineering A* **493** (1–2), 104 (2008).
3. R.B. Figueiredo, T.G. Langdon. *Advanced Engineering Materials* **10** (1-2), 37-40 (2008).
4. H.K. Lin, J.C. Huang. *Materials Transactions* **43** (10), 2424 (2002).
5. H.K. Lin, J.C. Huang, T.G. Langdon. *Materials Science and Engineering A* **402**, 250 (2005).
6. R.B. Figueiredo, T.G. Langdon. *Materials Science and Engineering A* **501**, 105 (2009).
7. A. Mohan, W.Yuan, R.S. Mishra. *Materials Science and Engineering A* **562**, 69 (2013).
8. J. Stráská, M. Janeček, J. Čížek, J. Stráský, B. Hadzima. *Materials Characterization* **94**, 69 (2014).
9. E.W. Hart. *Acta Metallurgica* **15**, 351 (1967).
10. A. Considère, *Ann. Ponts Chauss. (Set. 6)*. **9**, 574 (1885).
11. T.G. Langdon. *Metallurgical Transactions A* **13** (5), 689 (1982).
12. P. Haehner. *Acta Metall, Mater.* **43** (11), 4093 (1995).
13. P. Málek. *Materials Science and Engineering A* **137**, 21 (1991).
14. J. Vrátná, M. Janeček, J. Čížek, D.J. Lee, E.Y. Yoon, H.S. Kim. *Journal of Materials Science* **48** (13), 4705 (2013).
15. M. Janeček, J. Čížek, J. Gubicza, J. Vrátná. *Journal of Materials Science* **47** (22), 7860 (2012).
16. H. J. Frost, M. F. Ashby. *Deformation-mechanism maps: the plasticity and creep of metals and ceramics*. Pergamon Press, New York, ISBN 0080293387 (1982).
17. M.F. Ashby, R.A. Verrall. *Acta Metallurgica* **21**, 149 (1973).
18. J.P. Young, H. Askari, Y. Hovanski, M.J. Heiden, D.P. Field. *Materials Characterization* **101**, 9 (2015).
19. A. Molinari, J. Méc. Théor. Appl. **4**, 659 (1985).